

1           Various evolutionary trajectories lead to loss of the tobramycin-  
2           potentiating activity of the quorum sensing inhibitor baicalin hydrate in

3                                   *Burkholderia cenocepacia* biofilms

4  
5           Andrea Sass<sup>a,\*</sup>, Lisa Slachmuylders<sup>a,\*</sup>, Heleen Van Acker<sup>a</sup>, Ian Vandebussche<sup>a</sup>, Lisa Ostyn<sup>a</sup>,  
6           Aurélie Crabbé<sup>a</sup>, Laurent Chiarelli<sup>b</sup>, Silvia Buroni<sup>b</sup>, Filip Van Nieuwerburgh<sup>c</sup>, Emmanuel  
7                                   Abatih<sup>d</sup>, Tom Coenye<sup>a</sup>

8  
9           <sup>a</sup>Laboratory of Pharmaceutical Microbiology, Ghent University, Ghent, Belgium

10          <sup>b</sup>Department of Biology and Biotechnology, University of Pavia, Pavia, Italy

11          <sup>c</sup>Laboratory of Pharmaceutical Biotechnology, Ghent University, Ghent, Belgium

12          <sup>d</sup>FIRE Unit, Department of Applied Mathematics, Computer Sciences and Statistics, Ghent University,  
13          Ghent, Belgium

14          \* Both authors contributed equally

15  
16          Address correspondence to Tom Coenye, Tom.Coenye@UGent.be

17  
18          Running title: Evolution of resistance to a potentiator in *B. cenocepacia* biofilms

19  
20

## 21 **Abstract**

22 Combining antibiotics with potentiators that increase their activity is a promising strategy to tackle  
23 infections caused by antibiotic-resistant and -tolerant bacteria. As these potentiators typically do not  
24 interfere with essential processes of bacteria, it has been hypothesized that they are less likely to  
25 induce resistance than conventional antibiotics. However, evidence supporting this hypothesis is  
26 lacking. In the present study, we investigated whether *Burkholderia cenocepacia* J2315 biofilms  
27 develop resistance towards one such adjuvant, baicalin hydrate (BH), a quorum sensing inhibitor  
28 known to increase antibiotic-induced oxidative stress. Biofilms were repeatedly and intermittently  
29 treated with tobramycin (TOB) alone or in combination with BH for 24 h. After each cycle of  
30 treatment, the remaining cells were quantified using plate counting. After 15 cycles, biofilm cells  
31 were less susceptible to treatments with TOB and TOB+BH, compared to the start population, and  
32 the potentiating effect of BH towards TOB was lost. Whole genome sequencing was performed to  
33 probe which changes were involved in the reduced effect of BH and mutations in 14 protein-coding  
34 genes were identified (including mutations in genes involved in central metabolism and in BCAL0296,  
35 encoding an ABC transporter), as well as a partial deletion of two larger regions. No changes in the  
36 minimal inhibitory or minimal bactericidal concentration of TOB or changes in the number of  
37 persister cells were observed in the evolved populations. However, basal intracellular levels of  
38 reactive oxygen species (ROS) and ROS levels found after treatment with TOB were markedly  
39 decreased in the evolved populations. In addition, in evolved cultures with mutations in BCAL0296, a  
40 significantly reduced uptake of TOB was observed. Our results indicate that resistance towards  
41 antibiotic-potentiating activity can develop rapidly in *B. cenocepacia* J2315 biofilms and point to  
42 changes in central metabolism, reduced ROS production, and reduced TOB uptake as potential  
43 mechanisms.

44

45

## 46 **Importance**

47 Bacteria show a markedly reduced susceptibility to antibiotics when growing in a biofilm, which  
48 hampers effective treatment of biofilm-related infections. The use of potentiators that increase the  
49 activity of antibiotics against biofilms has been proposed as a solution to this problem, but it is  
50 unclear whether resistance to these potentiators could develop. Using an experimental evolution  
51 approach, we convincingly demonstrate that *Burkholderia cenocepacia* biofilms rapidly develop  
52 resistance towards the tobramycin-potentiating activity of baicalin hydrate. Whole genome  
53 sequencing revealed that there are different mechanisms that lead to this resistance, including  
54 mutations resulting in metabolic changes, changes in production of intracellular levels of reactive  
55 oxygen species, and differences in transporter-mediated tobramycin uptake. Our study suggests that  
56 this form of combination therapy is not 'evolution-proof' and highlights the usefulness of  
57 experimental evolution to identify mechanisms of resistance and tolerance in biofilm-grown bacteria.

58

59

## 60 Introduction

61 Due to increasing levels of antimicrobial resistance, novel strategies to tackle bacterial infections are  
62 needed and an interesting approach is the use of antibiotic adjuvants or potentiators. Potentiators  
63 are compounds with little or no antibacterial activity that interfere with bacterial resistance  
64 mechanisms and/or increase antimicrobial activity when co-administered with an antibiotic (1-5). A  
65 well-known class of antibiotic adjuvants are quorum sensing (QS) inhibitors (QSIs) (6). QSIs target the  
66 cell-density based bacterial communication network that regulates the expression of multiple  
67 virulence factors (7, 8). Whether resistance would develop towards these adjuvants is currently  
68 unknown and QSIs have long been accepted as 'evolution-proof': as QSIs do not target pathways  
69 essential for growth, it has been hypothesized that development of resistance would not occur (or at  
70 least would occur less frequently), due to the lack of selective pressure favouring the rise of resistant  
71 mutants (9-13). However, natural selection occurs when heritable variation provides a fitness  
72 advantage and QS disruption can affect bacterial fitness in conditions in which a functional QS system  
73 is essential (8). This was for example shown by cultivating *Pseudomonas aeruginosa* in medium with  
74 adenosine as a sole carbon source (14). As growth on adenosine depends on the production of a  
75 nucleoside hydrolase, which is positively regulated by the key QS signal receptor LasR, a functional  
76 QS system is required for the growth of *P. aeruginosa* in these conditions (15). After addition of the  
77 brominated furanone C-30 (a known QSI), growth of *P. aeruginosa* on adenosine was impaired,  
78 resulting in selective pressure and the occurrence of resistant mutants. Adding this QSI caused  
79 mutations in repressor genes of the multidrug resistance efflux pump MexAB-OrpM, which resulted  
80 in an increased resistance towards C-30 (14). In clinical isolates of cystic fibrosis (CF) patients never  
81 exposed to C-30, mutations in the same genes were found, leading to reduced susceptibility to C-30  
82 (14, 16). Based on these results, Maeda et al speculated that any strong selective pressure can induce  
83 resistance to antivirulence compounds (14, 17). In clinical practice, these adjuvants would be co-  
84 administered with an antibiotic. This means selective pressure imposed by this antibiotic needs to be  
85 included in the experimental set up when investigating possible development of resistance towards

86 the adjuvants (1, 2). In addition, while most evolutionary studies on the development of resistance  
87 are carried out with planktonic cells (18-20), 65-80% of all infections are thought to be biofilm-  
88 related, and biofilm-associated bacteria typically show a reduced susceptibility towards antimicrobial  
89 agents (21).

90 *Burkholderia cenocepacia* is an opportunistic pathogen that causes severe lung infections in people  
91 with CF, which can further develop into a life-threatening systemic infection known as the cepacia  
92 syndrome (22). Antimicrobial therapy in CF often fails due to high innate resistance of *B. cenocepacia*  
93 towards many antibacterial agents and high tolerance associated with its biofilm-lifestyle (22, 23).  
94 Previously, several adjuvants were identified that increased the activity of tobramycin (TOB) (an  
95 aminoglycoside antibiotic frequently used in CF lung infections) (24) towards *B. cenocepacia* biofilms,  
96 including the QSI baicalin hydrate (BH) (6, 25).

97 The goal of the present study is to evaluate whether (and how) *B. cenocepacia* J2315 biofilm cells can  
98 develop resistance towards the TOB-potentiating activity of BH. To this end we used a slightly  
99 modified form of a previously-described bead-based biofilm assay (26) in which *B. cenocepacia* J2315  
100 cells were repeatedly and intermittently exposed to TOB, TOB+BH or a control treatment (Fig. 1).

101

## 102 **Results and discussion**

### 103 **Experimental evolution**

104 Three lineages of *B. cenocepacia* J2315 cells were repeatedly and intermittently exposed to TOB,  
105 TOB+BH or a control treatment (Fig. 1). After 24 h of growth on the beads, LIVE/DEAD staining was  
106 performed to evaluate biofilm formation (Fig. S1). A dense biofilm was formed in the cavity of the  
107 doughnut-shaped bead (rather than on the exterior sides of the bead) with approximately  
108  $10^7$  CFU/bead (prior to treatment).

109 The number of log(CFU/bead) after every cycle is shown in Fig. 2 and Table S1. After fitting a linear  
110 mixed-effect model (LMEM) (using log(CFU/bead) as the dependent variable and cycle, treatment,  
111 lineage and their two- and three-way interactions as fixed effects) and plotting the residuals against

112 the corresponding fitted values, no departures from the main assumptions of normality and  
113 constancy of error variance were found. The remaining models were fit for each lineage separately  
114 following significance of the three way interaction effect and residuals were assessed for each of the  
115 models for each lineage. An overview of the statistical results obtained can be found in Tables 1 and  
116 S2.

117 At the start of the evolution experiment, cells were more susceptible to the TOB+BH combination  
118 than to TOB alone, confirming that BH potentiates the activity of TOB against biofilms, as previously  
119 shown (6, 27). Over time, biofilm-grown *B. cenocepacia* J2315 cells became gradually less susceptible  
120 to the treatment (both to treatment with TOB alone and to the TOB+BH combination treatment); this  
121 occurred in all three lineages (Fig. 2). Evolution towards reduced susceptibility occurred significantly  
122 faster with the combined TOB+BH treatment, than for the TOB treatment (lineage 1:  $p = 0.0075$ ;  
123 lineage 2 and 3:  $p < 0.0001$ ) (Table 1) and our data indicate that in all lineages, the TOB-potentiating  
124 activity of BH was lost after 15 cycles, i.e. treatment with the combination TOB + BH was not able to  
125 kill more cells than treatment with TOB alone (Fig. S2).

126

## 127 **Genome analysis**

128 To investigate the reason behind this decreased susceptibility, whole genome sequencing was  
129 performed. The results are summarised in Table 2. When considering all (nine) evolved lines, changes  
130 in 18 protein-coding genes were observed, as well as a partial deletion of two larger regions. Some  
131 changes were common and appeared in all evolved cultures at the same location (e.g. changes in  
132 BCAL1315, BCAL1664 and BCAM0949); we speculate these mutations were already present in the  
133 start population at low frequency and were enriched for during the experimental evolution. Other  
134 changes occurred only in one or a few samples (e.g. mutations in BCAL0929, BCAL2476a, BCAM1901)  
135 and likely arose during the evolution study. For several genes that were mutated in multiple evolved  
136 cultures we noticed the occurrence of different types of mutations (e.g. BCAL0269, BCAL1525,  
137 BCAM0965).

138 All evolved cultures had mutations in the 5' untranslated region (UTR) of BCAL1525 (either a single  
139 SNP or insertion of a transposase at variable locations, Table 2). BCAL1525 encodes an Flp pilus  
140 assembly protein and has a 307 nt long and strongly expressed 5'UTR with multiple transcription  
141 start sites (TSS) (28). BCAL1525 to BCAL1536 seem to form an operon with Flp pilus genes, although  
142 there is a terminator at position 1690709 to 1690746 between BCAL1525 and BCAL1526, and no  
143 further downstream TSS could be identified (28). Flp pili belong to the type IVb pilus family (29),  
144 which is poorly characterized in *Burkholderia* species. In *P. aeruginosa* type IV pili are thought to play  
145 a role in biofilm formation (30), although recent data suggest this may depend on the biofilm model  
146 system used (31). Mutations in BCAL1525 occur at high frequency in all evolved cultures, irrespective  
147 of the treatment, suggesting there is an evolutionary pressure to lose the pilus function in the given  
148 experimental conditions. As biofilm formation is not affected in the course of the experiment, this  
149 indicates the Flp pilus is not required for biofilm formation in these conditions.

150 BCAL0296 encodes for both the transmembrane and nucleotide binding domains of an ABC transport  
151 protein and it is the only gene which is mutated in all treated evolved populations (except for one  
152 evolved population treated with TOB) but not in the control evolved populations; three different  
153 types of mutations are observed in this gene (a deletion, a nonsense mutation and a non-  
154 synonymous substitution, Table 2).

155 Three mutated genes are related to central metabolism and occur in TOB+BH treated lineages only.  
156 BCAL2631 and BCAM0965 are both involved in oxaloacetate production. The mutation in BCAL2631  
157 occurs only in one population exposed to TOB+BH; this gene encodes phosphoenol pyruvate kinase,  
158 which converts phosphoenol pyruvate to oxaloacetate in the 'reverse TCA cycle'. Its activity typically  
159 results in increased oxaloacetate levels and an increased flux through the TCA cycle (32). It was  
160 designated as conditionally essential in *B. cenocepacia* J2315 in a minimal medium with only glucose  
161 as substrate (33). BCAM0965 (encoding malate dehydrogenase) is mutated in two out of three  
162 evolved populations exposed to TOB+BH. Just like phosphoenol pyruvate kinase, malate  
163 dehydrogenase (which converts malate to oxaloacetate) activity will increase cellular oxaloacetate

164 levels, likely stimulating the TCA cycle. BCAM0965 is also conditionally essential in *B. cenocepacia*  
165 J2315 (33). On top of that, in one TOB+BH exposed evolved population, a mutation in a gene  
166 encoding the permease of a glucose/mannose ABC transporter (BCAL3040) was observed, likely  
167 affecting uptake of certain carbohydrates.

168 None of the mutations observed were located in genes known to be responsible for aminoglycoside  
169 resistance such as genes encoding for aminoglycoside-modifying enzymes, efflux pumps, or ribosome  
170 methyltransferases, or in genes encoding for ribosomal RNAs (34, 35). Since mutations in these genes  
171 often come at the cost of reduced relative growth fitness (36), the re-growth phase between  
172 treatment cycles might have prevented accumulation of such mutations.

173

#### 174 **Role of QS and QSI**

175 BH was previously described as a QSI (6), and in a recent study we showed it also has QS-  
176 independent activities, including modulating the oxidative stress response, that potentiate TOB in *B.*  
177 *cenocepacia* (27). To evaluate whether BH directly inhibits the *N*-octanoyl-L-homoserine lactone  
178 synthase Ceps (37, 38), an enzymatic assay with purified Ceps was carried out. Ceps enzymatic activity  
179 was first tested at the concentration of BH slightly below that used for the evolution study (200  $\mu$ M)  
180 and at this concentration BH completely inhibits Ceps; subsequently, the IC<sub>50</sub> was determined (46.8  $\pm$   
181 6.8  $\mu$ M) which confirmed that BH inhibits Ceps in a concentration dependent way (Fig. S3).

182 The mutation in BCAM1870, coding for Ceps, is found in two evolved populations exposed to TOB+BH  
183 and in a single population exposed to TOB only; the same mutation (C131W) is found in these three  
184 populations. Using qPCR, we investigated the expression of *ceps* (BCAM1870) and two QS-regulated  
185 genes (*aidA* [BCAS0293] and *zmpA* [BCAS0409]) (38) in cultures derived from the TOB-exposed  
186 biofilm of lineage 2. In stationary phase expression levels of these genes were not altered, but lower  
187 expression levels for these genes were observed in late log-phase cultures of the *ceps* mutant, with  
188 remarkably low levels of *aidA* expression (approx. 60-fold lower expression compared to the control)



189 (Fig. 3). This confirms that QS is indeed affected in this mutant. How the mutation in *cepl* contributes  
190 to an increased fitness of the evolved *B. cenocepacia* populations is currently unknown.

191

## 192 **Phenotypic characterisation of evolved lines**

193 The lack of mutations in known TOB resistance genes suggested that the overall gradual decrease in  
194 susceptibility of *B. cenocepacia* J2315 biofilm cells treated with TOB alone is not caused by a  
195 resistance mechanism specific for TOB. This is in line with the MIC and MBC values for TOB obtained  
196 for the different lineages (Table 3): in the presence or absence of BH, MIC and MBC values for TOB in  
197 the evolved lines are equal to or within one 2-fold dilution of the values obtained for the start  
198 culture.

199 Secondly, we determined whether the evolutionary changes affected the number of persister cells in  
200 treated cultures (experiments concerning persisters were carried out in two-fold with lineage 3 only).  
201 Persisters are known to occur in *B. cenocepacia* biofilms (39) and mutations leading to an increased  
202 fraction of persisters could (at least partially) explain the reduced effect of TOB+BH in the evolved  
203 lineages. However, the fraction of persisters recovered from *B. cenocepacia* J2315 biofilms after  
204 exposure to 4xMIC TOB were low and very similar for the control (0.0224%), the culture evolved in  
205 the presence of TOB (0.0393%) and the culture evolved in the presence of TOB+BH (0.0548%), ruling  
206 out increased persister formation as a source for the diminishing effect of TOB+BH (Fig. S4).

207 Planktonic growth rate was not affected in any of the lineages evolved in the presence of TOB, but a  
208 slightly reduced growth rate was observed for lineages 1 and 2 evolved in the presence of TOB+BH  
209 (Fig. S5). This reduction in growth was most pronounced for lineage 2, particularly in early  
210 exponential and stationary growth phase. Interestingly, this is also the only lineage that has  
211 mutations in two conditionally essential genes (BCAL2631 and BCAM0965) (33), potentially  
212 explaining this growth phenotype.

213 Subsequently, we investigated whether there were differences in production of reactive oxygen  
214 species (ROS) between the start culture and the evolved populations. We have previously shown that

215 bactericidal antibiotics (including TOB) induce ROS in *B. cenocepacia* biofilms and that this  
216 contributes to the antibiotic-mediated killing in *B. cenocepacia* (39-41). In addition, we have  
217 previously shown that BH increases TOB-induced oxidative stress in a QS-independent way (27). ROS  
218 are an inevitable by-product of aerobic respiration and as we observed mutations in genes involved  
219 in oxaloacetate production (BCAL2631 and BCAM0695) or glucose/mannose transport (BCAL3040) in  
220 all lineages treated with TOB+BH (but not in lineages treated with TOB alone or in control lineages,  
221 Table 2) we hypothesised these mutations could affect ROS levels. First, we investigated if basal ROS  
222 levels (i.e. ROS levels observed in the absence of a treatment with a bactericidal antibiotic) were  
223 different between the start culture and the evolved populations. For the control populations and  
224 populations treated with TOB, significantly increased basal ROS levels were observed in two and one  
225 of the lineages, respectively (Fig. 4A). For two of the populations that evolved in the presence of  
226 TOB+BH, a significant decrease in basal ROS production was observed ( $p < 0.05$ ) (Fig. 4A). These were  
227 also the populations in which mutations in BCAL2631 and/or BCAM0965 (thought to co-regulate TCA  
228 activity) were observed. When ROS levels were determined after exposure to TOB, increased ROS  
229 production was observed for one of the control populations while no significant difference was  
230 observed for any of the populations evolved in the presence of TOB alone ( $p < 0.05$ ) (Fig. 4B). All  
231 populations evolved in the presence of TOB+BH showed reduced ROS levels compared to the start  
232 culture after treatment with TOB; this difference was significant ( $p < 0.05$ ) for two lineages (Fig. 4B).  
233 Homologues of the putative ABC transporter BCAL0296, mutated in most evolved treated  
234 populations (but not in the controls), have been characterised in other bacteria. In *Bradyrhizobium*  
235 sp. the transporter homologue BclA is involved in protection against stress by antimicrobial peptides  
236 (42). BclA has multidrug transport activity and is involved in uptake of peptide-derived/peptide-like  
237 compounds, including bleomycin (43). The homologue in *Mycobacterium tuberculosis* is involved in  
238 uptake of vitamin B<sub>12</sub> and bleomycin (44). It is therefore possible that BCAL0296 can import TOB into  
239 the cytoplasm under the experimental conditions used. To investigate this, we used a flow cytometry  
240 based assay to determine uptake of BODIPY-conjugated TOB. While there are no statistically

241 significant differences when all nine groups (three lineages, three treatments) are compared (Fig. S6),  
242 differences in TOB uptake become apparent between treatments when data for the three  
243 treatments are averaged over the different lineages (Fig. 6), with TOB uptake significantly higher in  
244 the evolved control lines than in the evolved lines exposed to TOB ( $p = 0.045$ ) or TOB+BH ( $p < 0.001$ ).  
245 No significant difference was observed between the TOB and the TOB+BH exposed cultures. The  
246 results from this assay show that there is a significantly higher fraction of the population positive for  
247 BODIPY-TOB in evolved cultures without a mutation in BCAL0296 (i.e. the controls), than in evolved  
248 cultures with a mutation in BCAL0296 (i.e. the ones exposed to TOB or TOB+BH) (Fig. 5). These data  
249 suggest that BCAL0296 is involved in TOB import in *B. cenocepacia* and that the mutations occurring  
250 after repeated exposure to TOB or TOB+BH contribute to the reduced antimicrobial activity of TOB  
251 observed.

252

## 253 **Conclusion**

254 In the present study we demonstrate that during experimental evolution *in vitro*, *B. cenocepacia*  
255 J2315 biofilms gradually but quickly become less susceptible to TOB, and that evolution towards  
256 reduced susceptibility occurs significantly faster with the combined TOB+BH treatment. Many  
257 genetic changes were observed in the evolved populations exposed to the combination of TOB and  
258 BH, and some point to modifications in metabolism as a mechanism underlying the reduced  
259 susceptibility. The reduced levels of ROS (both basal levels and levels induced after exposure to TOB)  
260 observed in the lineages treated with TOB+BH point in the same direction. In addition, most lineages  
261 exposed to TOB or TOB+BH had mutations in BCAL0296, encoding an ABC transporter. Cells from  
262 populations in which BCAL0296 was mutated were more likely to accumulate lower levels of TOB  
263 intracellularly, providing an additional explanation for the reduced susceptibility of these evolved  
264 lineages. Although some genetic changes were found in multiple evolved populations, different  
265 lineages exposed to the same treatment appeared to have used different evolutionary trajectories to  
266 counteract the potentiating activity of BH. Our results indicate that resistance to potentiators can

267 develop in multiple ways and this might limit their clinical applicability. Finally, our data demonstrate  
268 that experimental evolution combined with high-throughput sequencing can indeed identify the  
269 genetic changes behind reduced susceptibility, and allows to identify hitherto unknown genes of  
270 interest likely involved in *B. cenocepacia* biofilm resistance and tolerance (45).

271

## 272 **Materials and methods**

### 273 **Strains and culture conditions**

274 *B. cenocepacia* J2315 (LMG 16656) was stored at -80°C using Microbank vials (Prolab Diagnostics,  
275 Richmond Hill, ON, Canada) and subcultured at 37°C on Trypton Soy agar (TSA; Lab M, Lancashire,  
276 UK). Overnight cultures were grown aerobically in Mueller Hinton broth (MHB; Lab M) at 37°C.

277

### 278 **Reagents**

279 Tobramycin (TOB; TCI Europe, Zwijndrecht, Belgium) was dissolved in physiological saline (PS) (0.9 %  
280 w/v NaCl) (Applichem, Darmstadt, Germany), filter sterilized (0.22 µm Whatman, Dassel, Germany)  
281 and stored at 4°C until use. Stock solutions of BH (Sigma-Aldrich, Bornem, Belgium) were prepared in  
282 dimethyl sulfoxide (DMSO; Sigma-Aldrich) and diluted in PS prior to use.

283

### 284 **Biofilm formation on beads**

285 The set-up for biofilm formation was inspired by that reported by Traverse et al. (26). Cryobeads  
286 from Microbank vials (Prolab Diagnostics) were used as substrates for biofilm formation. The beads  
287 were rinsed with PS prior to use to remove the cryopreservative present in the Microbank vials. This  
288 was achieved by adding 1 ml PS, vortexing the vial, removing the PS and repeating this three times.  
289 Six beads were then transferred to the wells of a 24-well microtiter plate (MTP, SPL Lifescience,  
290 Korea) and one ml of a diluted overnight culture of *B. cenocepacia* J2315 (containing approximately 5  
291 x 10<sup>7</sup> colony forming units (CFU) per ml) was used as inoculum. The MTP was statically incubated at  
292 37°C for 24 hours. To evaluate the ability of *B. cenocepacia* J2315 cells to form mature biofilms on

293 the beads, Live/Dead staining (LIVE/DEAD BacLight bacterial viability kit, Thermo Fischer Scientific,  
294 Invitrogen, Carlsbad, CA, USA) was performed after 24 hours of biofilm formation. The biofilms on  
295 the beads were visualized using an EVOS FL Auto Cell Imaging System (Thermo Fischer Scientific,  
296 Waltham, MA, USA) (Syto9:  $\lambda_{\text{ex}} = 470/22 \text{ nm}$ ,  $\lambda_{\text{em}} = 510/42 \text{ nm}$ ; propidium iodide:  $\lambda_{\text{ex}} = 531/40 \text{ nm}$ ;  
297  $\lambda_{\text{em}} = 593/40 \text{ nm}$ ).

298

## 299 **Evolution experiment**

300 To evaluate the influence of repeated treatments on biofilm susceptibility, cells were exposed to  
301 15 cycles of biofilm formation (24 h), treatment (24 h), and planktonic regrowth (48 h) (Fig. 1). The  
302 planktonic regrowth step was included to generate a sufficiently high number of cells to set up a new  
303 biofilm for the next cycle. Biofilms were treated with PS (untreated control), TOB alone (at a  
304 concentration of 768  $\mu\text{g/ml}$  which equals 3 times the minimal inhibitory concentration [MIC]), and  
305 TOB in combination with BH (250  $\mu\text{M}$ ). The concentration of TOB and BH was selected based on  
306 preliminary experiments: the concentrations used in the present study lead to a significant reduction  
307 in cell numbers compared to the untreated control, but not complete eradication, so that regrowth  
308 in the following cycles can occur. Three independent experiments (designated as lineages) were set  
309 up for each condition, i.e. TOB (tobramycin), TOB+BH, and an untreated control. The three lineages  
310 were started from three different overnight start cultures. Biofilms were grown as described above  
311 and after 24 hours the beads were rinsed with PS and treated with TOB or a combination of TOB +  
312 BH. After 24 hours of treatment at 37°C, the supernatant was removed, and the beads were rinsed  
313 with PS. Each well contained 6 beads: two beads were transferred to Eppendorf tubes containing 8%  
314 dimethyl sulfoxide (DMSO; Sigma-Aldrich) in MH for storage at -80°C, while the four remaining beads  
315 were transferred to a Falcon tube containing 8 ml MH medium. Sessile cells were detached from the  
316 beads by three cycles of vortexing (1 min, Vortex-Genie 2, Scientific Industries Inc., Bohemia, NY,  
317 USA) and sonicating (1 min; Branson 3510, Branson Ultrasonics Corp, Danbury, CT, USA). Six ml of  
318 this bacterial suspension was transferred to another tube and was incubated for 48 h for regrowth,

319 while shaking at 250 rpm at 37°C (KS 4000i control, IKA Works, Wilmington, NC, USA). The remaining  
320 2 ml was used to determine the number of surviving cells per bead (CFU/bead) by plating.

321

322 **Determination of the minimal inhibitory concentration (MIC) and minimum bactericidal**  
323 **concentration (MBC)**

324 To verify if possible changes in susceptibility over time were due to increased resistance towards  
325 TOB, the MIC and MBC for TOB was determined for the start and end population. MICs were  
326 determined according to the EUCAST broth microdilution assay using flat-bottom 96-well microtiter  
327 plates (MTP; SPL Lifescience, Korea) (46). The MIC was defined as the lowest concentration with a  
328 similar optical density as uninoculated growth medium. Absorbance was measured at 590 nm with a  
329 multilabel MTP reader (EnVision, Perkin Elmer LAS, Waltham, MA). All MIC determinations were  
330 performed in duplicate. The MBC was determined by plating the suspension used for the MIC test  
331 and the MBC was the lowest concentration that did not allow recovery of colonies following 48h  
332 incubation at 37°C.

333

334 **Determination of the number of persisters in tobramycin-exposed *B. cenocepacia* J2315 biofilms**

335 To determine whether the evolutionary changes affected persistence, the number of persisters  
336 surviving TOB treatment was compared between biofilms formed by the start and evolved cultures.  
337 Biofilms were grown in 96 well microtiter plates as described previously (47) and exposed for 24 h to  
338 TOB in a concentration of 4 × MIC (1024 µg/ml) (39). Briefly, an inoculum suspension containing 5 ×  
339 10<sup>7</sup> CFU/ml was added to the wells of a round bottomed 96 well microtiter plate. Following 4 h of  
340 adhesion, the supernatant was removed, and the plates were rinsed with PS. Subsequently, 100 µl of  
341 fresh MHB was added, and the plates were further incubated at 37 °C. After 24 h, the supernatant  
342 was removed and 120 µl of a TOB solution in PS or 120 µl PS (= control) was added. After 24 h, cells  
343 were harvested by vortexing and sonication (2 × 5 min) (Branson 3510, Branson Ultrasonics Corp,

344 Danbury, CT) and quantified by plating on LBA. Ten wells were included per strain, and the  
345 experiment was repeated twice. ( $n = 3$ ).

346

### 347 **Measurement of ROS levels**

348 To investigate whether there were differences in the production of reactive oxygen species (ROS)  
349 between the start culture and the evolved lineages, ROS was measured in treated and untreated  
350 start and evolved cultures. To measure ROS planktonic cultures were exposed to 2',7'-  
351 dichlorodihydrofluorescein diacetate (H2DCFDA) in a final concentration of 10  $\mu$ M in LB Broth (40).  
352 After 45 min of incubation protected from light, cells were washed with PBS and treated with TOB in  
353 a concentration of 4 x MIC or pH-matched phosphate buffered saline (PBS) (= untreated control  
354 solution with the same pH as the antibiotic solution) for 24 h. Fluorescence ( $\lambda$  excitation = 485 nm,  $\lambda$   
355 emission = 535 nm) was measured using an Envision plate reader. Autofluorescence of bacterial cells  
356 incubated without the probe and background fluorescence of the buffer solutions was measured and  
357 taken into account when calculating the net fluorescence. For the planktonic cultures an overnight  
358 culture was diluted to an optical density of 0.1 (approximately  $10^8$  cells/ml). After an additional 24 h  
359 of growth in a shaking warm water bath, cell suspensions with an optical density of 1 (approximately  
360  $10^9$  cells/ml) were transferred to falcon tubes and centrifuged for 9 min at 3634 rcf. Cells were  
361 resuspended in fresh medium with or without dye to measure ROS. Five wells were included per  
362 condition and the experiment was repeated twice ( $n = 3 \times 5$ ).

363

### 364 **Genome sequencing and data analysis**

365 After planktonic regrowth of the cells, DNA was extracted using a modified bead-beater protocol,  
366 adapted from Mahenthiralingam et al. (48). RNase-treated DNA was then quantified using the  
367 BioDrop  $\mu$ LITE (BioDrop, Cambridge, UK). Genomic DNA from the start culture and all evolved  
368 cultures obtained after 15 cycles were sequenced. Libraries were prepared using the NEBNext kit  
369 from Illumina, and sequenced either on an Illumina Nextseq 500 or HiSeq 4000, generating 150 bp

370 paired-end reads (Table S3). The experimental protocols and the raw sequencing data of all samples  
371 can be found in ArrayExpress under the accession number E-MTAB-6236. Sequenced reads were  
372 quality trimmed (error probability limit 0.05) and mapped to the *B. cenocepacia* J2315 reference  
373 genome (34) using CLC Genomics Workbench version 11.0.1. (Qiagen, Aarhus, Denmark) with a cut-  
374 off of 80% for similarity and 50% mapped read length. Mapping parameters were: match score 1,  
375 mismatch cost 2, insertion and deletion cost 3. More than 98.6% of reads mapped to the reference  
376 genome for all samples (Table S3). The un-mapped reads were *de-novo* assembled in CLC Genomics  
377 Workbench, but no contigs with a coverage >10% of the average coverage of the respective sample  
378 were found and gene acquisition was therefore excluded. In CLC Genomics Workbench, the InDels  
379 and Structural Variants tool was used to detect insertions and deletions, with a p-value threshold of  
380 0.0001. The output was manually screened on mapping patterns of un-aligned read ends and only  
381 entries with a single breakpoint and identical sequences in the un-aligned read ends were reported.  
382 The consensus sequence of the un-aligned read ends was then used to confirm the deletion or to  
383 identify the nature of the inserted sequence. A larger insertion sequence cannot be fully deduced in  
384 this manner, but only a certain type of transposase which was already present multiple times in the  
385 *B. cenocepacia* J2315 reference genome was detected: *Burkholderia cepacia* insertion element IS407.  
386 Both consensus sequences at insertion breakpoints were consistent with either end of this  
387 transposase, it was therefore concluded that the insertion consisted of only that transposase. The  
388 Basic Variant Detection tool was used to detect Single Nucleotide Polymorphisms (SNPs) with a  
389 minimum coverage of 10 and a reference-to-variant ratio of 35%. This was the lowest cut-off that  
390 allowed to clearly distinguish true SNPs from sequencing errors. All SNPs were then manually  
391 screened for false positives in regions containing repetitive sequences or hairpins, which caused poor  
392 mapping. The function of the genes that acquired mutational changes was determined using the  
393 Conserved Domain database (49) and *Burkholderia* Genome Database (50).

394

395 **qPCR**



396 Cultures from cycle 15, control lineage 3 and Tob lineage 2, were cultivated in MHB in a shaking  
397 incubator at 150 rpm for 6 to 10 hours. Late log phase cultures were harvested at a density of 1 - 1.3  
398  $\times 10^9$  CFU/ml and stationary phase cultures at a density of 3 - 4.5  $\times 10^9$  CFU/ml. Cell pellets were  
399 frozen at -80°C and RNA was extracted within one week of harvest, using the RiboPure bacteria kit  
400 (Thermo Fisher, Rochester, NY, USA), according to the standard protocol, including DNase treatment.  
401 RNA was quantified with the BioDrop  $\mu$ LITE. cDNA was generated with the High Capacity cDNA  
402 Reverse Transcription kit (Applied Biosystems, Foster City, CA, USA), from 500 ng of RNA. qPCR was  
403 performed in a CFX96 Real-Time System C1000 Thermal Cycler (Bio-Rad, Hercules, CA, USA) using  
404 GoTaq qPCR Master Mix (Promega, Madison, WI, USA). Cq values were normalised against a  
405 previously-validated control gene (*rpoD*, BCAM0918) (51, 52). Fold changes were calculated  
406 compared to a standard (mix of all cDNAs in experiment) and log-transformed. Primers are listed in  
407 Table S4.

408

#### 409 **Growth curves**

410 Growth curves were determined in MHB. 200  $\mu$ l/well of a 5  $\times 10^5$  CFU/ml inoculum was added in  
411 triplicates to a round-bottom MTP and the absorbance at 590 nm was measured in a microplate  
412 reader (Envision, Perkin Elmer, Shelton, CT, USA), every 30 minutes for 50 hours. The experiment was  
413 repeated 3 times and representative curves are shown.

414

#### 415 **Determination of Ceps activity in the presence of BH**

416 *B. cenocepacia* Ceps was expressed in *Escherichia coli* BL21(DE3) cells and purified according to the  
417 procedure previously described (53). Enzymatic activity was determined by a spectrophotometric  
418 assay, according to Christensen *et al.* (54), which measures the *holo*-ACP formation by titrating the  
419 release of the free thiol of ACP with dichlorophenylindophenol (DCPIP;  $\epsilon = 19100 \text{ M}^{-1} \text{ cm}^{-1}$ ).  
420 Measurements were performed at 37 °C, in a final volume of 100  $\mu$ l, using an Eppendorf  
421 Biospectrometer. The standard reaction mixture contained 50 mM HEPES pH 7.5, 0.005% Nonidet P-

422 40, 0.13 mM DCPIP, 70  $\mu$ M Octanoyl-ACP (C8-ACP) (55, 56) and 4  $\mu$ M CepI; the reactions were  
423 started by addition of 40  $\mu$ M S-adenosyl methionine (SAM), after pre-incubation for 10 min. CepI  
424 inhibition was initially screened at 200  $\mu$ M of BH (dissolved in DMSO). CepI inhibition was initially  
425 screened at 200  $\mu$ M (dissolved in DMSO) and subsequently the IC<sub>50</sub> was determined by measuring  
426 enzyme activities in presence of different BH concentrations, and fitting data according to equation  
427 (1):

$$428 \quad A_{[I]} = A_{[0]} \times \left(10 \frac{[I]}{[I] + IC_{50}}\right) \quad \text{equation (1)}$$

429 where A<sub>[I]</sub> is the enzyme activity at BH concentration [I] and A<sub>[0]</sub> is the enzyme activity without BH. All  
430 measurements were performed in triplicate.

431

#### 432 **Quantification of intracellular tobramycin levels**

433 BODIPY-labelled tobramycin was synthesized as previously described (57). Bacteria were grown  
434 under biofilm-forming conditions for 4 h in MHB in the presence of 0.75  $\mu$ g/mL BODIPY-tobramycin  
435 at 37 °C. Following 4 h of biofilm formation, the biofilm was rinsed to remove extracellular  
436 tobramycin, homogenized and subjected to flow cytometry analysis (Attune NxT, Life Technologies).  
437 The bacterial population was delineated based on the forward and side scatter signal, and a  
438 threshold was set to exclude non-cellular particles and cell debris. BODIPY-tobramycin that  
439 associated with bacterial cells was determined through excitation with a 488 nm laser. Fluorescence  
440 emission was detected through a 530/30 bandpass filter. Controls included bacterial biofilm cells that  
441 were not exposed to BODIPY-tobramycin (negative control) or to incremental levels of tobramycin to  
442 determine the concentration at which saturation was obtained. Based on the negative control and  
443 the concentration of tobramycin where maximal population saturation was obtained, negative and  
444 positive flow cytometry gates were determined respectively. At least 10,000 bacteria were analysed  
445 per sample.

446

#### 447 **Statistical analysis**

448 To determine whether the observed variations in survival over time for the different treatments  
449 were statistically significant, a linear mixed-effect model (LMEM) was used. The model uses  
450 log(CFU/bead) as the dependent variable and cycle, treatment, lineage and their two- and three-way  
451 interactions as fixed effects and was fit using SAS version 9.4 (SAS institute, Cary, NC, USA). To  
452 account for possible correlations between the measurements over cycles, a compound symmetry  
453 variance covariance structure was used. All interaction effects that were not significant were  
454 excluded from the model. When an interaction was significant, this was considered as the fixed effect  
455 to evaluate differences in treatment effect. Per lineage, treatments were compared pairwise to TOB  
456 treatment using the Tukey adjustment method. Assumptions associated with the LMEM were  
457 checked based on residuals from the fitted final model (Table S2).

458 Other data sets were analysed using SPSS version 25 software (SPSS, Chicago, IL, USA). The Shapiro-  
459 Wilk test was used to verify the normal distribution assumption of the data. Normally distributed  
460 data were analysed using a one-way ANOVA, while non-normally distributed data were analysed with  
461 a Kruskal-Wallis 1-way ANOVA. P-values smaller than 0.05 were considered statistically significant.

462

## 463 **Funding**

464 This work was supported by the Special Research Fund of Ghent University (grant number  
465 BOF13/24j/017); the Belgian Science Policy Office (grant P7/28 of the Interuniversity Attraction Pole  
466 program); and by the Fund for Scientific Research (postdoctoral fellowship to HVA and Odysseus  
467 fellowship to AC).

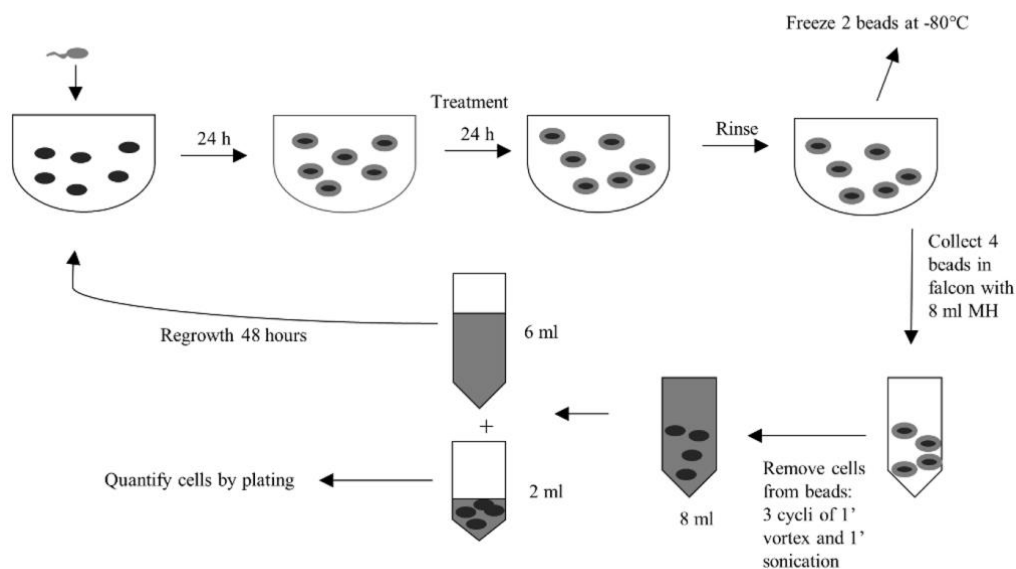
468

469

470

471 **Figures**

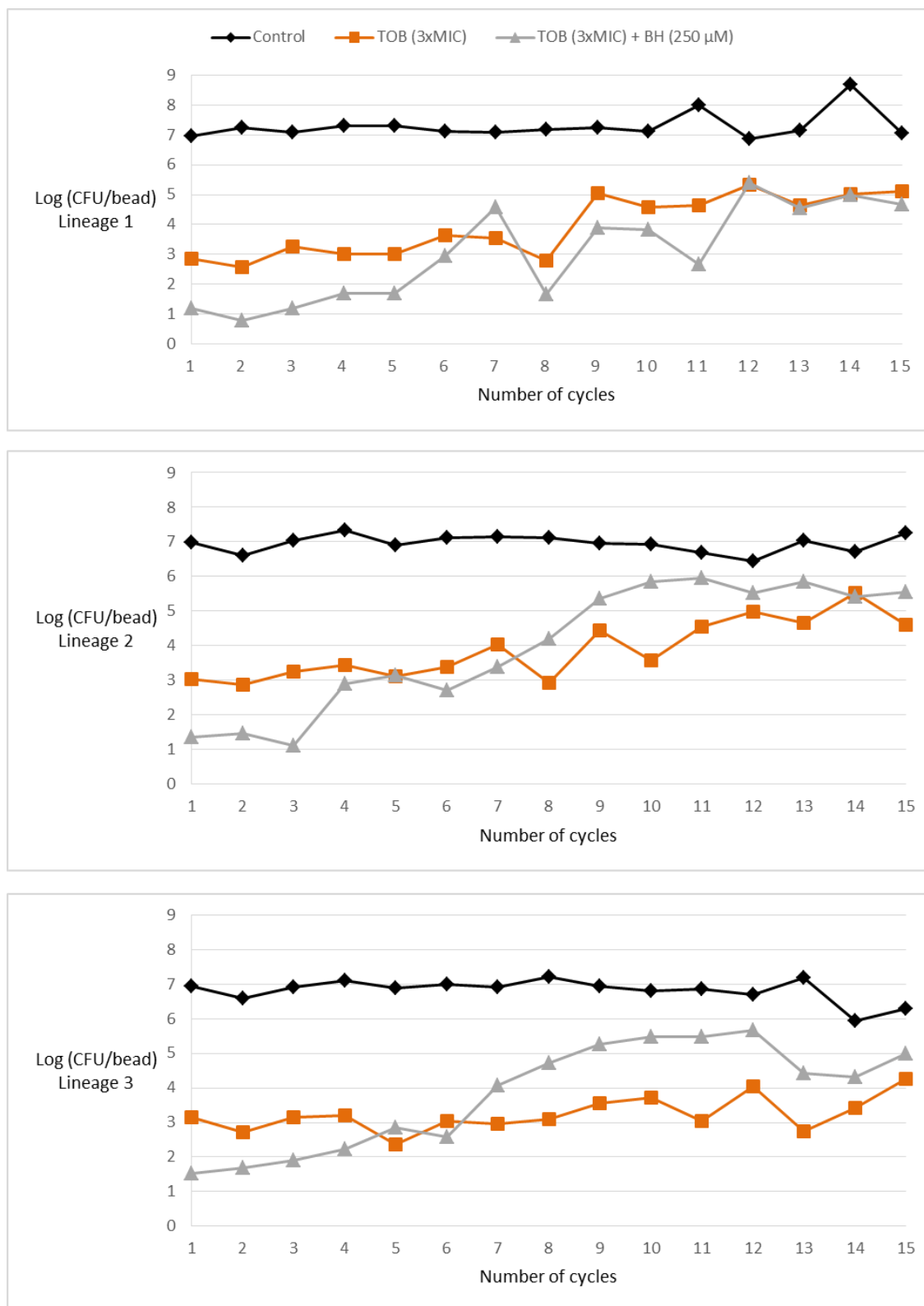
472 **FIG 1** Experimental set up. Fresh inoculum (grey) is added to six cryobeads (black full circles) in each  
473 well of a 24-well microtiter plate. After 24 hours, mature biofilms (grey circles) are formed on the  
474 surface of the beads. These biofilms are treated for 24 hours. Afterwards, the supernatant is  
475 removed, and the beads are rinsed with PS. Two beads, containing a mature biofilm, are stored at -  
476 80°C. The four other beads are transferred to a falcon tube, in which the sessile cells from the beads  
477 are harvested. A part of these cells is used for quantification, while another part is used for  
478 planktonic regrowth of the cells (48 hours).



479

480

481 **FIG 2** Number of *B. cenocepacia* J2315 biofilm cells, expressed as log(CFU/bead), in the untreated  
482 control (Control) and after repeated treatments with TOB or TOB+BH.

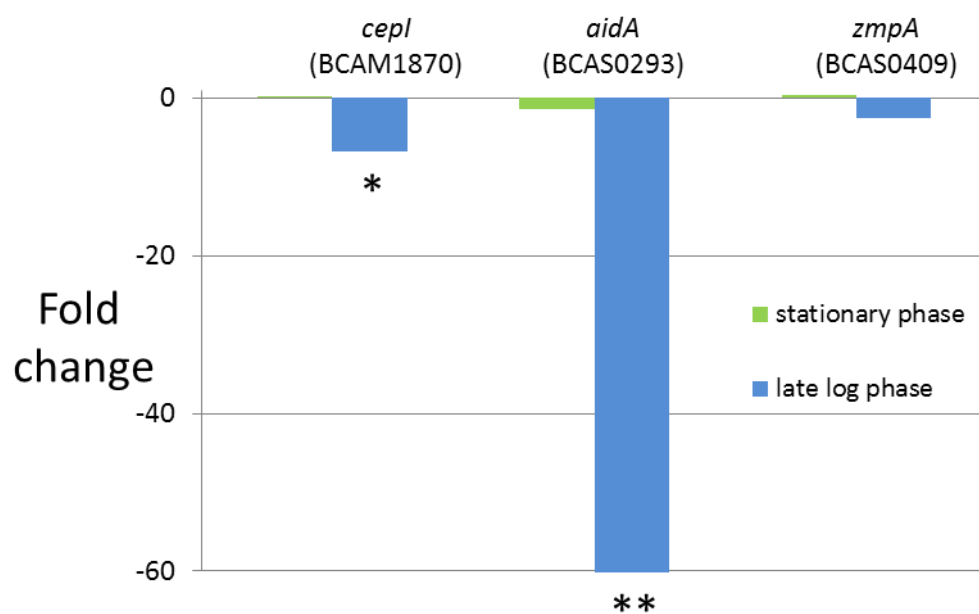


483

484

485 **FIG 3** Expression of *cepl*, *aidA* and *zmpA* in TOB-exposed evolved lineage compared to control  
486 lineage, as determined by qPCR. Data shown are fold change in TOB-exposed lineage compared to  
487 control. \*,  $p < 0.05$ ; \*\*,  $p < 0.01$ .

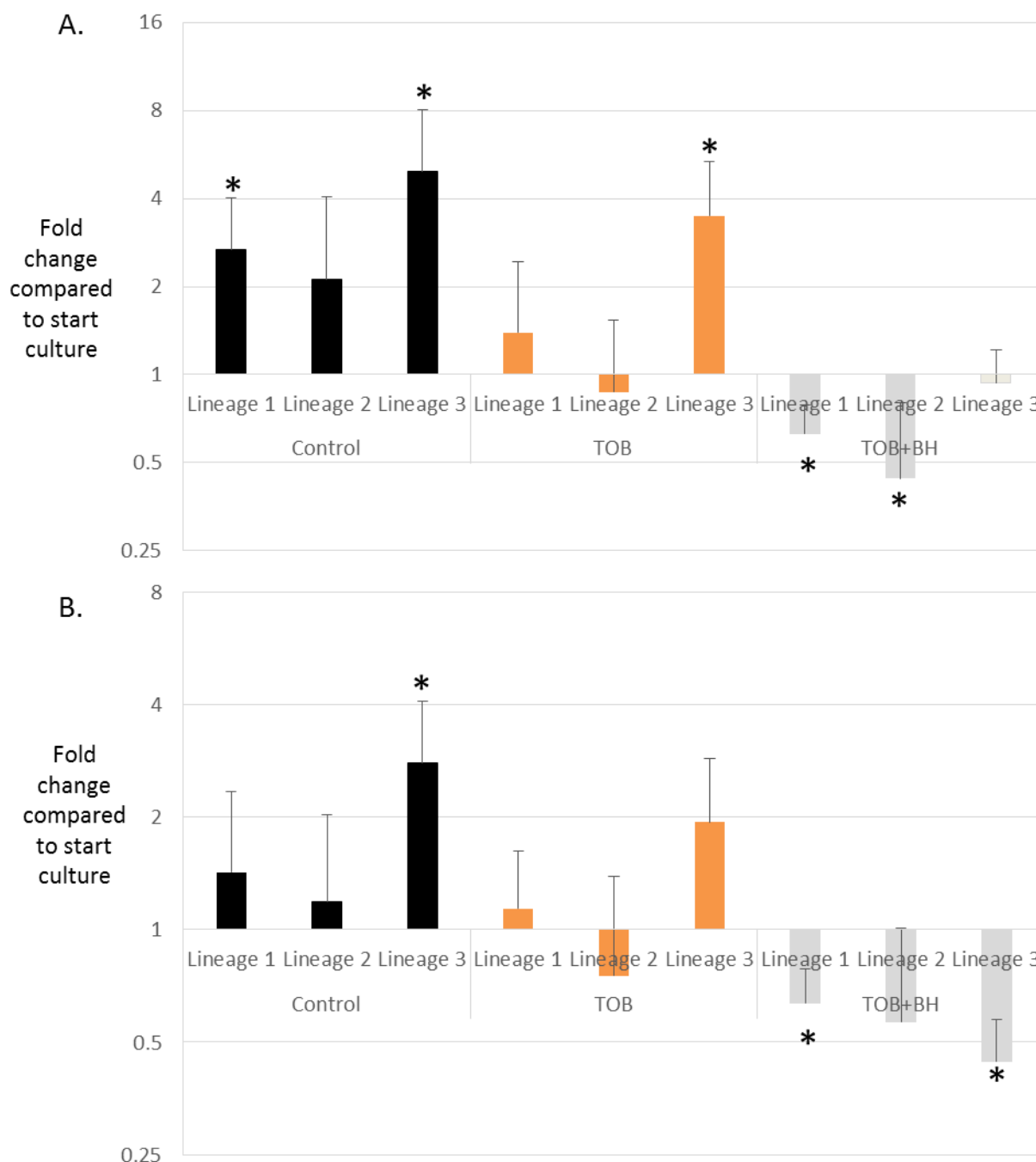
488



489

490

491 **FIG 4 A.** Basal ROS levels in evolved populations (relative compared to start culture). B. ROS levels in  
492 evolved populations after exposure to 4xMIC TOB (relative compared to start culture). Data shown  
493 are averages and error bars represent standard error (n = 3 x 5). Statistically significant differences (p  
494 < 0.05) are indicated by an asterisk.

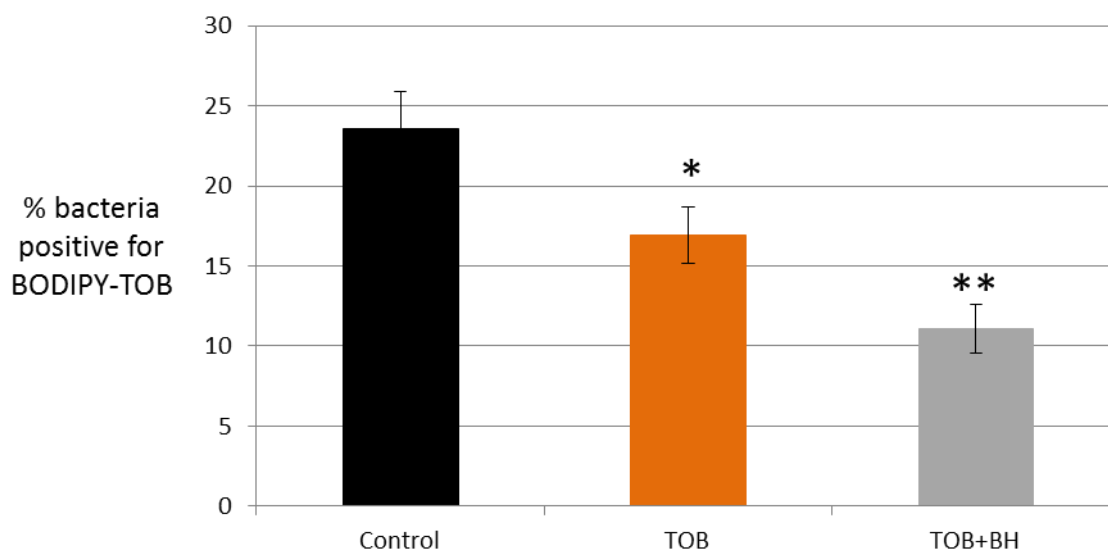


495

496

497

498 **FIG 5** Differences in TOB uptake between treatments (based on averaged data over the different  
499 lineages). Data shown are average, error bars indicate standard error (n=24). \*, p < 0.05; \*\*, p < 0.001



500

501



502 **Tables**

503 **TABLE 1** Most important results of the LMEM per lineage. Treatments were pairwise compared to

504 TOB treatment over time.

	<b>Factor</b>	<b>t value</b>	<b>Tukey adjusted p-value</b>
<b>Lineage 1</b>	Untreated control	-4.09	<0.0001
	TOB+BH	2.71	0.0075
<b>Lineage 2</b>	Untreated control	-4.41	<0.0001
	TOB+BH	6.13	<0.0001
<b>Lineage 3</b>	Untreated control	-2.49	0.0139
	TOB+BH	6.08	<0.0001

505 **TABLE 2** Mutations observed in evolved populations. Numbers represent variant-to-reference ratios.

506

Gene designation	Function	Type	Start culture	Contr 1	Contr 2	Contr 3	TOB 1	TOB 2	TOB 3	TOB+BH 1	TOB+BH 2	TOB+BH 3
BCAL0296	ABC transporter component, peptide transporter	Deletion from BCAL0294 to BCAL0296 (328273 to 330830)					91					
BCAL0296	ABC transporter component, peptide transporter	Stop codon in CDS (330739 G to T, S331STOP)					100 <sup>a</sup>	99		100	100	
BCAL0296	ABC transporter component, peptide transporter	SNP in CDS (330925 A to T, I269N)										100
BCAL0736	PTS system EI component, carbohydrate transport	Deletion in CDS, 18 bp, 2 different locations, both in frame			100	91			98			
BCAL0929	DeoR family glycerol-3-phosphate regulon repressor, GlpR	Deletion in CDS (10 bp 1012042..1012051)		100								
BCAL1172	Conserved hypothetical protein, in BcenGI5	Deletion of first 148 bp of gene		100								92
BCAL1315	Conserved hypothetical protein, in BcenGI6	Transposase inserted in CDS, same location	21	99	98	97	98	95	96	96	97	97
BCAL1525	Flp pilus assembly protein	SNP in 5'UTR (1690247 G to C)			96							
BCAL1525	Flp pilus assembly protein	Transposase(s) inserted in 5'UTR at various locations <sup>b</sup>		96		79	97	94	100	29	96	94
BCAL1664	Conserved hypothetical protein	SNP in 5'UTR (1818909 G to A)	51	100	100	100	100	100	100	100	100	100
BCAL2476a	Conserved hypothetical protein fragment, in	Transposase inserted in 5'UTR		97								

	BcenGI8											
BCAL2628	Heme biosynthesis-associated TPR protein	Stop codon in CDS (2889248 C to A, E232STOP)		96	89		77					
BCAL2631	Phosphoenolpyruvate carboxylase	2 SNPs in CDS (2895340..2895341 GC to TT, R724C)								81		
BCAL3040	ABC-type sugar transport system, permease component	SNP in CDS (3332415 A to G, F51L)									100	
BCAM0821	Methyl-accepting chemotaxis protein	SNP in CDS (907087 G to T, A369C)			52							
BCAM0949	Exported lipase LipA	SNP in CDS (1051105 C to G, S180W)	47	100	100	100	100	100	100	100	100	100
BCAM0965	Malate dehydrogenase	SNP in CDS (1070727 C to G, W254C)								58		
BCAM0965	Malate dehydrogenase	Stop codon in CDS (1070776 G to T, S238STOP)									100	
BCAM1204	Alanine racemase, catabolic	SNP in 5'UTR (1316206 C to T)									100	
BCAM1870	Cepl	SNP in CDS (2088576 C to G, C131W)					99		99		100	
BCAM1901	Hypothetical phage protein	Transposase inserted in CDS									93	
BCAM2284	Enolase	SNP in CDS (2566450 G to A, P103S)		100	99		99					
BCAL1017 - BCAL1028	Includes diguanylate cyclase BCAL1020	Partial deletion of duplicated region <sup>c</sup>	20	100	100	100	100	100	100	100	100	100
BCAL2581 - BCAL2591		Partial deletion of BcenGI8	50	100	100	100	100	100	100	100	100	100

508 <sup>a</sup> The region is deleted in 91% of the population, the remaining 9% all have a SNP in this gene

509 <sup>b</sup> Insertion sites of transposase in 5'UTR of BCAL1525: Control 1, TB2, TB3: after 1690210; Control 3: two insertion sites after 1690218 (35%) and 1690239  
510 (34%); Control 3: two insertion sites after 1690218 (35%) and 1690239 (34%); TOB1: after 1690239; TOB2: after 1690196; TOB3: five insertion sites after  
511 1690196, 1690206, 1690210, 1690218 and 1690239; TBH1: two insertion sites after 1690196 (15%) and 1690228 (14%). Orientation of transposase is  
512 variable.

513 <sup>c</sup> The deleted genes are still present in the genome, but no longer duplicated.

514

515

516 **TABLE 3** MIC and MBC of TOB in *B. cenocepacia* J2315 recovered from different samples. MIC and  
517 MBC were determined in presence (TOB+BH) and absence (TOB) of BH.

	<b>Treatment</b>	<b>MIC of TOB (<math>\mu\text{g/ml}</math>)</b>	<b>MBC of TOB (<math>\mu\text{g/ml}</math>)</b>
Start culture	TOB	256	256
	TOB+BH	256	256
Lineage 1, treated with TOB	TOB	128	128
	TOB+BH	128	128
Lineage 1, treated with TOB+BH	TOB	256	256
	TOB+BH	128	256
Lineage 2, treated with TOB	TOB	128	128
	TOB+BH	128	128
Lineage 2, treated with TOB+BH	TOB	128	128
	TOB+BH	128	128
Lineage 3, treated with TOB	TOB	256	256
	TOB+BH	256	256
Lineage 3, treated with TOB+BH	TOB	256	512
	TOB+BH	512	512

518

519

520

521 **REFERENCES**

522

- 523 1. Gill EE, Franco OL, Hancock RE. 2015. Antibiotic adjuvants: diverse strategies for controlling  
524 drug-resistant pathogens. *Chemical biology & drug design* 85:56-78.
- 525 2. Bernal P, Molina-Santiago C, Daddaoua A, Llamas MA. 2013. Antibiotic adjuvants:  
526 identification and clinical use. *Microbial biotechnology* 6:445-9.
- 527 3. Brown D. 2015. Antibiotic resistance breakers: can repurposed drugs fill the antibiotic  
528 discovery void? *Nature reviews Drug discovery* 14:821-32.
- 529 4. Brown ED, Wright GD. 2016. Antibacterial drug discovery in the resistance era. *Nature*  
530 529:336-43.
- 531 5. Wright GD. 2016. Antibiotic Adjuvants: Rescuing Antibiotics from Resistance. *Trends in*  
532 *microbiology* 24:862-871.
- 533 6. Brackman G, Cos P, Maes L, Nelis HJ, Coenye T. 2011. Quorum sensing inhibitors increase the  
534 susceptibility of bacterial biofilms to antibiotics in vitro and in vivo. *Antimicrobial agents and*  
535 *chemotherapy* 55:2655-61.
- 536 7. Waters CM, Bassler BL. 2005. Quorum sensing: cell-to-cell communication in bacteria. *Annual*  
537 *review of cell and developmental biology* 21:319-46.
- 538 8. Defoirdt T, Boon N, Bossier P. 2010. Can bacteria evolve resistance to quorum sensing  
539 disruption? *PLoS pathogens* 6:e1000989.
- 540 9. Melander RJ, Melander C. 2017. The Challenge of Overcoming Antibiotic Resistance: An  
541 Adjuvant Approach? *ACS infectious diseases* 3:559-563.
- 542 10. Hirakawa H, Tomita H. 2013. Interference of bacterial cell-to-cell communication: a new  
543 concept of antimicrobial chemotherapy breaks antibiotic resistance. *Frontiers in*  
544 *microbiology* 4:114.
- 545 11. Hentzer M, Wu H, Andersen JB, Riedel K, Rasmussen TB, Bagge N, Kumar N, Schembri MA,  
546 Song Z, Kristoffersen P, Manefield M, Costerton JW, Molin S, Eberl L, Steinberg P, Kjelleberg  
547 S, Hoiby N, Givskov M. 2003. Attenuation of *Pseudomonas aeruginosa* virulence by quorum  
548 sensing inhibitors. *The EMBO journal* 22:3803-15.
- 549 12. Gerdt JP, Blackwell HE. 2014. Competition studies confirm two major barriers that can  
550 preclude the spread of resistance to quorum-sensing inhibitors in bacteria. *ACS chemical*  
551 *biology* 9:2291-9.
- 552 13. Mellbye B, Schuster M. 2011. The sociomicrobiology of antivirulence drug resistance: a proof  
553 of concept. *mBio* 2.
- 554 14. Maeda T, Garcia-Contreras R, Pu M, Sheng L, Garcia LR, Tomas M, Wood TK. 2012. Quorum  
555 quenching quandary: resistance to antivirulence compounds. *The ISME journal* 6:493-501.
- 556 15. Heurlier K, Denervaud V, Haenni M, Guy L, Krishnapillai V, Haas D. 2005. Quorum-sensing-  
557 negative (*lasR*) mutants of *Pseudomonas aeruginosa* avoid cell lysis and death. *Journal of*  
558 *bacteriology* 187:4875-83.
- 559 16. Tomas M, Doumith M, Warner M, Turton JF, Beceiro A, Bou G, Livermore DM, Woodford N.  
560 2010. Efflux pumps, OprD porin, AmpC beta-lactamase, and multiresistance in *Pseudomonas*  
561 *aeruginosa* isolates from cystic fibrosis patients. *Antimicrobial agents and chemotherapy*  
562 54:2219-24.
- 563 17. Garcia-Contreras R, Maeda T, Wood TK. 2016. Can resistance against quorum-sensing  
564 interference be selected? *The ISME journal* 10:4-10.
- 565 18. Steenackers HP, Parijs I, Dubey A, Foster KR, Vanderleyden J. 2016. Experimental evolution in  
566 biofilm populations. *FEMS microbiology reviews* 40:373-97.
- 567 19. Van den Bergh B, Swings T, Fauvart M, Michiels J. 2018. Experimental Design, Population  
568 Dynamics, and Diversity in Microbial Experimental Evolution. *Microbiology and molecular*  
569 *biology reviews* : MMBR 82.

- 570 20. Zhang Q, Lambert G, Liao D, Kim H, Robin K, Tung CK, Pourmand N, Austin RH. 2011.  
571 Acceleration of emergence of bacterial antibiotic resistance in connected  
572 microenvironments. *Science (New York, NY)* 333:1764-7.
- 573 21. Van Acker H, Van Dijck P, Coenye T. 2014. Molecular mechanisms of antimicrobial tolerance  
574 and resistance in bacterial and fungal biofilms. *Trends in microbiology* 22:326-33.
- 575 22. Mahenthiralingam E, Urban TA, Goldberg JB. 2005. The multifarious, multireplicon  
576 *Burkholderia cepacia* complex. *Nature reviews Microbiology* 3:144-56.
- 577 23. Coenye T. 2010. Social interactions in the *Burkholderia cepacia* complex: biofilms and  
578 quorum sensing. *Future microbiology* 5:1087-99.
- 579 24. Scoffone VC, Chiarelli LR, Trespidi G, Mentasti M, Riccardi G, Buroni S. 2017. *Burkholderia*  
580 *cenoecepacia* Infections in Cystic Fibrosis Patients: Drug Resistance and Therapeutic  
581 Approaches. *Frontiers in microbiology* 8:1592.
- 582 25. Luo J, Dong B, Wang K, Cai S, Liu T, Cheng X, Lei D, Chen Y, Li Y, Kong J, Chen Y. 2017. Baicalin  
583 inhibits biofilm formation, attenuates the quorum sensing-controlled virulence and enhances  
584 *Pseudomonas aeruginosa* clearance in a mouse peritoneal implant infection model. *PloS one*  
585 12:e0176883.
- 586 26. Traverse CC, Mayo-Smith LM, Poltak SR, Cooper VS. 2013. Tangled bank of experimentally  
587 evolved *Burkholderia* biofilms reflects selection during chronic infections. *Proceedings of the*  
588 *National Academy of Sciences of the United States of America* 110:E250-9.
- 589 27. Slachmuylders L, Van Acker H, Brackman G, Sass A, Van Nieuwerburgh F, Coenye T. 2018.  
590 Elucidation of the mechanism behind the potentiating activity of baicalin against  
591 *Burkholderia cenoecepacia* biofilms. *PloS one* 13:e0190533.
- 592 28. Sass AM, Van Acker H, Forstner KU, Van Nieuwerburgh F, Deforce D, Vogel J, Coenye T. 2015.  
593 Genome-wide transcription start site profiling in biofilm-grown *Burkholderia cenoecepacia*  
594 J2315. *BMC genomics* 16:775.
- 595 29. Roux N, Spagnolo J, de Bentzmann S. 2012. Neglected but amazingly diverse type IVb pili.  
596 *Research in microbiology* 163:659-73.
- 597 30. Klausen M, Heydorn A, Ragas P, Lambertsen L, Aaes-Jorgensen A, Molin S, Tolker-Nielsen T.  
598 2003. Biofilm formation by *Pseudomonas aeruginosa* wild type, flagella and type IV pili  
599 mutants. *Molecular microbiology* 48:1511-24.
- 600 31. Davies EV, James CE, Brockhurst MA, Winstanley C. 2017. Evolutionary diversification of  
601 *Pseudomonas aeruginosa* in an artificial sputum model. *BMC microbiology* 17:3.
- 602 32. Sauer U, Eikmanns BJ. 2005. The PEP-pyruvate-oxaloacetate node as the switch point for  
603 carbon flux distribution in bacteria. *FEMS microbiology reviews* 29:765-94.
- 604 33. Wong YC, Abd El Ghany M, Naeem R, Lee KW, Tan YC, Pain A, Nathan S. 2016. Candidate  
605 Essential Genes in *Burkholderia cenoecepacia* J2315 Identified by Genome-Wide TraDIS.  
606 *Frontiers in microbiology* 7:1288.
- 607 34. Holden MT, Seth-Smith HM, Crossman LC, Sebahia M, Bentley SD, Cerdeno-Tarraga AM,  
608 Thomson NR, Bason N, Quail MA, Sharp S, Cherevach I, Churcher C, Goodhead I, Hauser H,  
609 Holroyd N, Mungall K, Scott P, Walker D, White B, Rose H, Iversen P, Mil-Homens D, Rocha  
610 EP, Fialho AM, Baldwin A, Dowson C, Barrell BG, Govan JR, Vandamme P, Hart CA,  
611 Mahenthiralingam E, Parkhill J. 2009. The genome of *Burkholderia cenoecepacia* J2315, an  
612 epidemic pathogen of cystic fibrosis patients. *Journal of bacteriology* 191:261-77.
- 613 35. Garneau-Tsodikova S, Labby KJ. 2016. Mechanisms of Resistance to Aminoglycoside  
614 Antibiotics: Overview and Perspectives. *MedChemComm* 7:11-27.
- 615 36. Hughes D, Andersson DI. 2017. Evolutionary Trajectories to Antibiotic Resistance. *Annual*  
616 *review of microbiology* 71:579-596.
- 617 37. Sokol PA, Sajjan U, Visser MB, Gingues S, Forstner J, Kooi C. 2003. The CepIR quorum-sensing  
618 system contributes to the virulence of *Burkholderia cenoecepacia* respiratory infections.  
619 *Microbiology (Reading, England)* 149:3649-58.

- 620 38. Subsin B, Chambers CE, Visser MB, Sokol PA. 2007. Identification of genes regulated by the  
621 cepI/R quorum-sensing system in *Burkholderia cenocepacia* by high-throughput screening of a  
622 random promoter library. *Journal of bacteriology* 189:968-79.
- 623 39. Van Acker H, Sass A, Bazzini S, De Roy K, Udine C, Messiaen T, Riccardi G, Boon N, Nelis HJ,  
624 Mahenthalingam E, Coenye T. 2013. Biofilm-grown *Burkholderia cepacia* complex cells  
625 survive antibiotic treatment by avoiding production of reactive oxygen species. *PLoS one*  
626 8:e58943.
- 627 40. Van Acker H, Gielis J, Acke M, Cools F, Cos P, Coenye T. 2016. The Role of Reactive Oxygen  
628 Species in Antibiotic-Induced Cell Death in *Burkholderia cepacia* Complex Bacteria. *PLoS one*  
629 11:e0159837.
- 630 41. Van Acker H, Coenye T. 2017. The Role of Reactive Oxygen Species in Antibiotic-Mediated  
631 Killing of Bacteria. *Trends in microbiology* 25:456-466.
- 632 42. Barriere Q, Guefrachi I, Gully D, Lamouche F, Pierre O, Fardoux J, Chaintreuil C, Alunni B,  
633 Timchenko T, Giraud E, Mergaert P. 2017. Integrated roles of BclA and DD-carboxypeptidase  
634 1 in *Bradyrhizobium* differentiation within NCR-producing and NCR-lacking root nodules.  
635 *Scientific reports* 7:9063.
- 636 43. Guefrachi I, Pierre O, Timchenko T, Alunni B, Barriere Q, Czernic P, Villaecija-Aguilar JA, Verly  
637 C, Bourge M, Fardoux J, Mars M, Kondorosi E, Giraud E, Mergaert P. 2015. *Bradyrhizobium*  
638 BclA Is a Peptide Transporter Required for Bacterial Differentiation in Symbiosis with  
639 *Aeschynomene* Legumes. *Molecular plant-microbe interactions : MPMI* 28:1155-66.
- 640 44. Gopinath K, Venclovas C, Ioerger TR, Sacchettini JC, McKinney JD, Mizrahi V, Warner DF.  
641 2013. A vitamin B(1)(2) transporter in *Mycobacterium tuberculosis*. *Open biology* 3:120175.
- 642 45. Cooper VS. 2018. Experimental Evolution as a High-Throughput Screen for Genetic  
643 Adaptations. *mSphere* 3.
- 644 46. (ESCMID) ECfASTEotESoCMaID. 2003. Determination of minimum inhibitory concentrations  
645 (MICs) of antibacterial agents by broth dilution *Clinical Microbiology and Infection* 9:ix-xv.
- 646 47. Van Acker H, Van Snick E, Nelis HJ, Coenye T. 2010. In vitro activity of temocillin against  
647 planktonic and sessile *Burkholderia cepacia* complex bacteria. *Journal of cystic fibrosis :*  
648 *official journal of the European Cystic Fibrosis Society* 9:450-4.
- 649 48. Mahenthalingam E, Campbell ME, Foster J, Lam JS, Speert DP. 1996. Random amplified  
650 polymorphic DNA typing of *Pseudomonas aeruginosa* isolates recovered from patients with  
651 cystic fibrosis. *Journal of clinical microbiology* 34:1129-35.
- 652 49. Marchler-Bauer A, Bo Y, Han L, He J, Lanczycki CJ, Lu S, Chitsaz F, Derbyshire MK, Geer RC,  
653 Gonzales NR, Gwadz M, Hurwitz DI, Lu F, Marchler GH, Song JS, Thanki N, Wang Z, Yamashita  
654 RA, Zhang D, Zheng C, Geer LY, Bryant SH. 2017. CDD/SPARCLE: functional classification of  
655 proteins via subfamily domain architectures. *Nucleic acids research* 45:D200-D203.
- 656 50. Winsor GL, Khaira B, Van Rossum T, Lo R, Whiteside MD, Brinkman FS. 2008. The  
657 *Burkholderia* Genome Database: facilitating flexible queries and comparative analyses.  
658 *Bioinformatics (Oxford, England)* 24:2803-4.
- 659 51. Sass AM, Schmerk C, Agnoli K, Norville PJ, Eberl L, Valvano MA, Mahenthalingam E. 2013.  
660 The unexpected discovery of a novel low-oxygen-activated locus for the anoxic persistence of  
661 *Burkholderia cenocepacia*. *The ISME journal* 7:1568-81.
- 662 52. Kiekens S, Sass A, Van Nieuwerburgh F, Deforce D, Coenye T. 2018. The Small RNA ncS35  
663 Regulates Growth in *Burkholderia cenocepacia* J2315. *mSphere* 3.
- 664 53. Scoffone VC, Chiarelli LR, Makarov V, Brackman G, Israyilova A, Azzalin A, Forneris F, Riabova  
665 O, Savina S, Coenye T, Riccardi G, Buroni S. 2016. Discovery of new diketopiperazines  
666 inhibiting *Burkholderia cenocepacia* quorum sensing in vitro and in vivo. *Scientific reports*  
667 6:32487.
- 668 54. Christensen QH, Grove TL, Booker SJ, Greenberg EP. 2013. A high-throughput screen for  
669 quorum-sensing inhibitors that target acyl-homoserine lactone synthases. *Proceedings of the*  
670 *National Academy of Sciences of the United States of America* 110:13815-20.



- 671 55. Cronan JE, Thomas J. 2009. Bacterial fatty acid synthesis and its relationships with polyketide  
672 synthetic pathways. *Methods in enzymology* 459:395-433.
- 673 56. Quadri LE, Weinreb PH, Lei M, Nakano MM, Zuber P, Walsh CT. 1998. Characterization of Sfp,  
674 a *Bacillus subtilis* phosphopantetheinyl transferase for peptidyl carrier protein domains in  
675 peptide synthetases. *Biochemistry* 37:1585-95.
- 676 57. Messiaen AS. 2013. Towards improvement of antibiotic therapy for treating *Burkholderia*  
677 *cepacia* complex biofilm infections in cystic fibrosis patients. PhD. Ghent University, Gent,  
678 Belgium.
- 679